Nanoscale

Accepted Manuscript

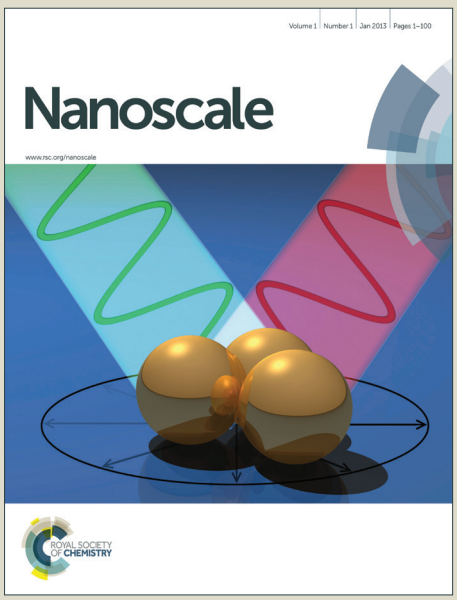

ROYAL SOCIETY OF CHEMISTRY

www.rsc.org/nanoscale

Journal Name

RSCPublishing

COMMUNICATION

Multifunctional Magnetic and Fluorescent Core-shell Nanoparticles for Bioimaging

Cite this: DOI: 10.1039/x0xx00000x

Yanjiao Lu,[a] Bicheng He,[b] Jie Shen,[b] Jie Li,[a] Wantai Yang [a] and Meizhen Yin*[a]

Received 00th January 2012,
Accepted 00th January 2012

DOI: 10.1039/x0xx00000x

www.rsc.org/

Novel magnetic and fluorescent core-shell nanoparticles have been fabricated, which exhibit superparamagnetic behavior and emit strong near-infrared fluorescence. The nanoparticles are highly biocompatible and can be internalized into cells with nucleic accumulation via strong interaction with nucleic acid, implying potential applications in biomedical fields.

The core-shell nanoparticles (NPs) have received increasing attention because of their improved physical and chemical properties over their single-component counterparts[1-4]. In particular, magnetic and fluorescent core-shell NPs represent one of the most exciting prospects in current biotechnology[5,6]. Since magnetic NPs have been widely used in magnetic resonance imaging[7-9], drug delivery[10] and hyperthermia applications[11, 12]. Moreover, the introduced fluorescence plays a particularly important role in chemical and biological sensing in cellular environments, such as bioimaging[13-16] or biolabelling[17, 18]. Near-infrared (NIR) fluorescent, multi-functional squarylium indocyanine dye containing four primary amines was selected in this work due to its water solubility and biocompatibility as well as non-overlap between its fluorescent peak and the cell autofluorescence[19]. Since the carboxymethyl chitosan (CMCS) has non-toxic nature, excellent biocompatibility and biodegradability[20, 21], the conjugated with CMCS on the surface of the NPs should be a good choice to explore the potential applications in biomedicine[22, 23]. Multifunctional biocompatible nanoparticles are expected to be fabricated for biomedical applications.

In this communication, highly fluorescent, magnetic and biocompatible core-shell NPs were prepared (Scheme 1). The core is Fe_3O_4 providing magnetic property. The first shell is SiO_2 coating which resistant the quenching of the fluorescence. The outmost shell is functionalized by CMCS and squarylium indocyanine dye (Cy5-NH_2)[19, 24]. The core-shell NPs with strong fluorescence and good biocompatibility can be internalized into the cells and accumulated in cell nuclei, which exhibit desirable capability for bioimaging.

Fe_3O_4 NPs with stable colloidal dispersion were prepared by co-precipitation method using oleic acid (OA) as surfactants[25]. Figure S1 displays the X-ray diffraction (XRD) pattern of the obtained Fe_3O_4 NPs. All detected diffraction peaks [(1 1 1), (2 0 0), (3 1 1), (2 2 2), (4 0 0), (4 2 2), (5 1 1), and (4 4 0)] of Fe_3O_4 in face centred cubic crystal (JCPDS card No. 19-0629) can be observed, indicating that Fe_3O_4 was synthesized successfully.

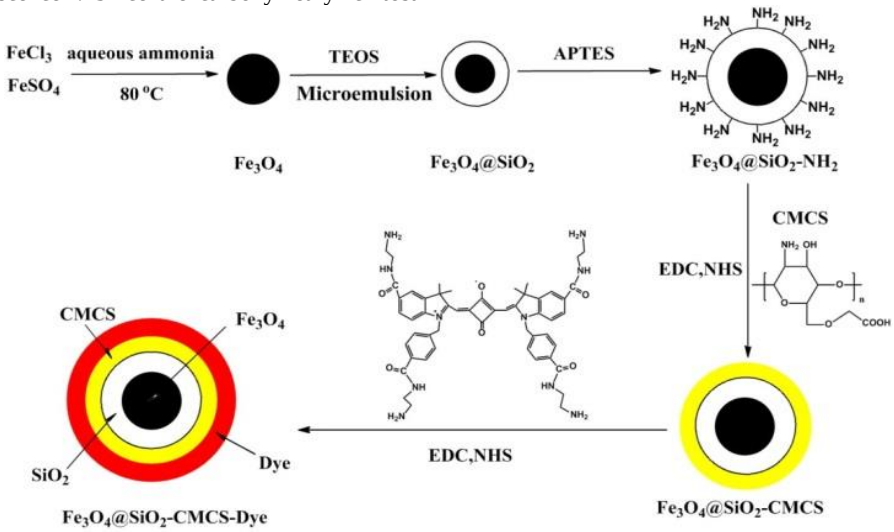

Scheme 1. Synthesis of multifunctional magnetic and fluorescent core-shell NPs.

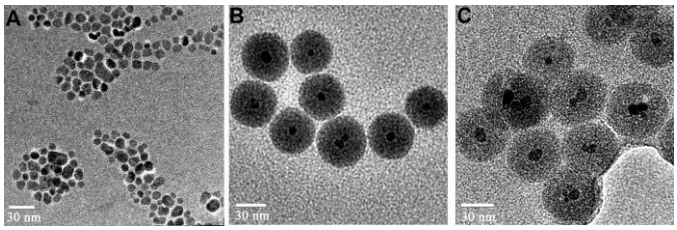

Figure 1. TEM images of (A) Fe_3O_4, (B) Fe_3O_4 @SiO_2 and (C) Fe_3O_4@SiO_2-NH-CMCS-Cy5 NPs.

To characterize the morphologies of prepared products, the aqueous dispersion of the black precipitates was treated with ultrasonication and then dropped onto a copper grid for high resolution transmission electron microscope (HRTEM) measurement. As shown in Figure 1A, the obtained Fe_3O_4 NPs have an average diameter of 10 nm. The silica-coated Fe_3O_4 NPs were prepared via a reverse microemulsion method. Figure 1B shows the TEM image of such Fe_3O_4@SiO_2 NPs. Monodispersed Fe_3O_4@SiO_2 NPs have nearly spherical core-shell structures with an average diameter of 46 nm. In most cases, each SiO_2 shell encapsulated only one Fe_3O_4 nanocrystal. Detailed synthesis procedures and material characterizations can be found in Electronic Supplementary Material (ESI).

The introduction of outer silica shell not only protects the inner magnetite core from oxidation but also provides reaction sites for further functionalization with amine groups by (3-aminopropyl) triethoxysilane (APTES). As shown in Figure S1, the modification of amine groups on the surface of NPs was proved by the chromogenic reaction with ninhydrin[26]. When ninhydrin was added into the solution, the color of the unmodified NPs (Fe_3O_4@SiO_2) solution shows slight yellow (Figure S2A). In contrast, the solution color of NPs modified with amine groups (Fe_3O_4@SiO_2-NH_2) turns blue after heating (Figure S2B), suggesting the successful introduction of primary amine groups on the surface of NPs.

In order to develop functionalized NPs for biomedical application, the surface functionalization of Fe_3O_4@SiO_2-NH_2 NPs with CMCS was performed via amidation. CMCS was first activated with N-(3-dimethylaminopropyl)-N′-ethylcarbodi imide (EDC) and N-hydroxysuccinimide (NHS), followed by coupling reaction with amine groups on the surface of Fe_3O_4@SiO_2-NH_2 NPs. The successful conjugation of CMCS on the NPs was characterized by FTIR (Figure S3) and XPS (Figure S4). The FTIR spectrum of Fe_3O_4@SiO_2-CMCS NPs (Figure S3B) shows not only the main characteristic band at 590 cm^{-1} owing to Fe-O stretching vibration (Figure S3A), but also the characteristic peaks at 1406 cm^{-1} due to C-N stretching[27] (Figure S3C). The results demonstrate that CMCS has been grafted onto the NPs successfully. Since the magnetic material disturb XPS signal, we also prepared SiO_2-CMCS NPs without Fe_3O_4 core, which were used for XPS measurement. Compared with the amine-modified SiO_2 (SiO_2-NH_2) NPs (Figure S4A), the CMCS conjugated NPs (Figure S4B) showed obvious increase of the C and N signal, indicating the successful introduction of CMCS on the NPs.

Similar to the above described procedure, the carboxyl group on the surface of Fe_3O_4@SiO_2-NH-CMCS NPs was activated with EDC/NHS and then reacted with amine-modified squarylium indocyanine dye (Cy5-NH_2)[28]. The TEM image of the Fe_3O_4@SiO_2-CMCS-Cy5 NPs is shown in Figure 1C. The Fe_3O_4@SiO_2-CMCS-Cy5 NPs are spherical and uniform in size, with an average diameter of 51 nm. Moreover, the surface organic group leaded to a rough outer surface, compared with the original surface of Fe_3O_4@SiO_2-NH_2 NPs. The absorption and emission of the product Fe_3O_4@SiO_2-CMCS-Cy5 NPs in water are shown in Figure 2. The maximum emission peak is located at 647 nm, which avoids much of the interference from biological autofluorescence. The magnetic property of the Fe_3O_4@ SiO_2-CMCS-Cy5 NPs was recorded using a VSM with fields up to 20 000 Oe. As shown in Figure 3, the saturation magnetization of Fe_3O_4@SiO_2-CMCS-Cy5 NPs was 8.19 emu g^{-1}, indicating that the composite NPs exhibit excellent superparamagnetism.

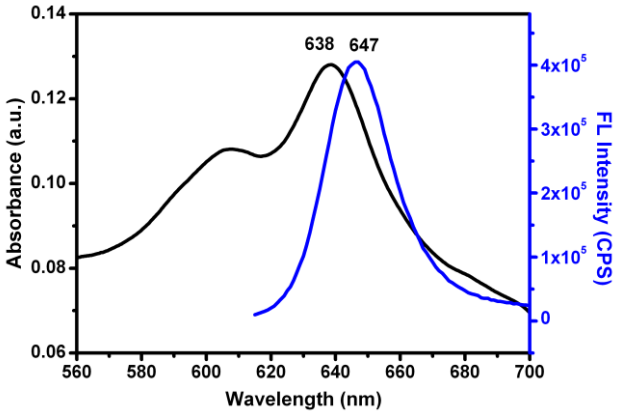

Figure 2. UV absorption and emission spectra of Fe_3O_4@SiO_2-CMCS-Cy5 NPs (0.1 mg/mL in water).

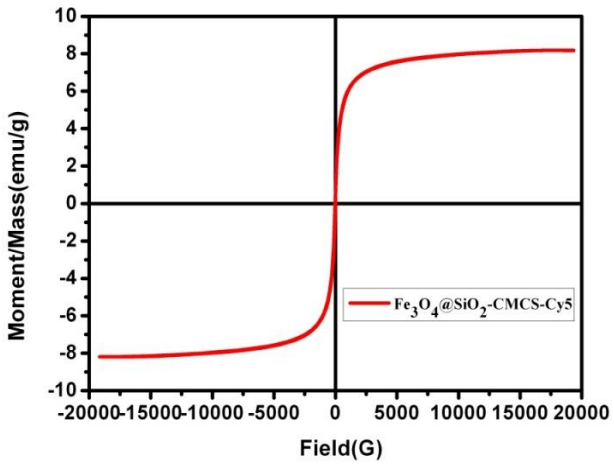

Figure 3. Hysteresis loop of the Fe_3O_4@SiO_2-CMCS-Cy5 NPs.

To verify the biocompatibility of the Fe_3O_4@SiO_2-CMCS-Cy5 NPs, cell cytotoxicity were assessed by the Tali™ viability assay. Figure S5 shows the concentration effect of Fe_3O_4@SiO_2-CMCS-Cy5 NPs on cell viability after incubation for 48 h. It indicates very high cell viability (>94%) even at a relatively high concentration of NPs (0.1 mg mL^{-1}). These results show that the Fe_3O_4@SiO_2-CMCS-Cy5 NPs have very low toxicity to live animal cells. Therefore, the NPs are suitable for potential applications in biomedicine.

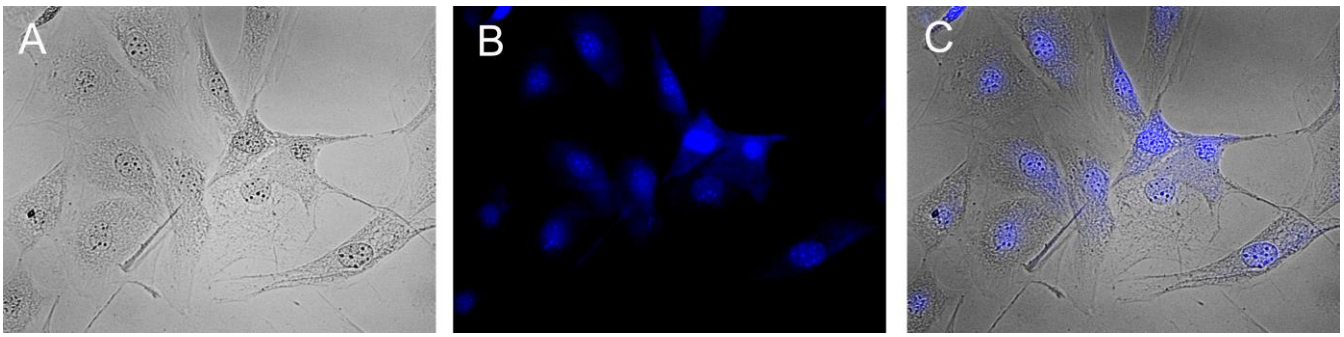

Figure 4. (A) Bright-field, (B) fluorescence, and (C) overlapping images of live cells stained with Fe_3O_4@SiO_2-CMCS-Cy5 NPs for 24 h.

Cellular uptake was carried out to investigate whether the Fe_3O_4@SiO_2-CMCS-Cy5 NPs can enter live cells. After incubation with 40 μg mL^{-1} of NPs for 24 h, the NPs can be internalized into the cells as demonstrated by the strong fluorescence of Cy5 within cells (Figure 4). The cellular internalization can be attributed to the endocytosis[29, 30]. It was reported that the Cy5-NH_2 dye can specifically stain the cell membrane structures of live tissues by interaction with the components of cell membrane[19]. Interestingly, the fluorescent image shows accumulation of Fe_3O_4@SiO_2-CMCS-Cy5 NPs in cell nuclei (Figure 4B). This might be attributed to the strong interaction between Fe_3O_4@SiO_2-CMCS-Cy5 NPs and DNA. In order to test the assumption, a direct interaction of the NPs with DNA (NPs/DNA) was revealed by spectral analysis (Figure S6). The emission intensity of NPs/DNA increased along with the DNA concentration at the excitation wavelength of 598 nm. Isothermal titration calorimetry (ITC) was used to further characterize the interaction of NPs/DNA. As shown in Figure S7, the measured affinity constant (K_A) of NPs with DNA was 4.6×10^6, suggesting the strong interaction. The ITC results and spectral analyses demonstrate the interaction of NPs/DNA. Therefore, the nanocomposites have distinct interaction with cellular, especially nuclear components, which deserves further investigation in future work.

Conclusions

In summary, we have successfully fabricated the multifunctional magnetic and fluorescent NPs with a clear core-shell structure where CMCS was conjugated on the surface. The composite NPs with a typical diameter of 51 ± 5 nm maintain a saturation magnetization of 8.19 emu g^{-1} at room temperature, and exhibit strong NIR fluorescence. Cell cytotoxicity assays revealed that the multifunctional NPs are highly biocompatible. Furthermore, the cell uptake experiments show that the core-shell NPs can be internalized into live cells with accumulation in cell nuclei. Spectral analysis and ITC demonstrated a strong interaction between the NPs and nucleic acid. These results imply the potential value for biomedical imaging and disease therapy.

Acknowledgement

This work was financially supported by the National Science Foundation of China (21174012, 51103008 and 51221002), the Beijing Natural Science Foundation (2142026), and the Doctoral Program of Higher Education Research Fund (20120010110008).

Notes and references

[a] State Key Laboratory of Chemical Resource Engineering, Key Laboratory of Carbon Fiber and Functional Polymers, Ministry of Education, Beijing Laboratory of Biomedical Materials, Beijing University of Chemical Technology, 100029 Beijing, China. Email: yinmz@mail.buct.edu.cn

[b] Department of Entomology, China Agricultural University, 100193 Beijing, China.

† Electronic Supplementary Information (ESI) available: See DOI: 10.1039/c000000x/

1. R. Ghosh Chaudhuri and S. Paria, *Chem. Rev.*, 2011, **112**, 2373-2433.
2. S. Wei, Q. Wang, J. Zhu, L. Sun, H. Lin and Z. Guo, *Nanoscale*, 2011, **3**, 4474-4502.
3. P. Zhang, Y. Huang, X. Lu, S. Zhang, J. Li, G. Wei and Z. Su, *Langmuir*, 2014, **30**, 8980-8989.
4. H. Wang, D. Sun, N. Zhao, X. Yang, Y. Shi, J. Li, Z. Su and G. Wei, *J. Mater. Chem. B*, 2014, **2**, 1362-1370.
5. N. Ž. Knežević, E. Ruiz-Hernández, W. E. Hennink and M. Vallet-Regí, *RSC Advances*, 2013, **3**, 9584-9593.
6. G. Wang and X. Su, *Analyst*, 2011, **136**, 1783-1798.
7. X. Zhao, H. Zhao, Z. Chen and M. Lan, *J. Nanosci. Nanotechnol.*, 2014, **14**, 210-220.
8. B. Y. W. Hsu, M. Wang, Y. Zhang, V. Vijayaragavan, S. Y. Wong, A. Y.-C. Chang, K. K. Bhakoo, X. Li and J. Wang, *Nanoscale*, 2014, **6**, 293-299.
9. H. Tan, J. M. Xue, B. Shuter, X. Li and J. Wang, *Adv. Funct. Mater.*, 2010, **20**, 722-731.
10. M. Namdeo, S. Saxena, R. Tankhiwale, M. Bajpai, Y. Mohan and S. Bajpai, *J. Nanosci. Nanotechnol.*, 2008, **8**, 3247-3271.
11. C. Grüttner, K. Müller, J. Teller and F. Westphal, *Int. J. Hyperthermia*, 2013, **29**, 777-789.
12. A. Salunkhe, V. Khot and S. Pawar, *Curr. Top. Med. Chem.*, 2014, 572-594.
13. S. K. Yen, D. Jańczewski, J. L. Lakshmi, S. B. Dolmanan, S. Tripathy, V. H. Ho, V. Vijayaragavan, A. Hariharan, P. Padmanabhan and K. K. Bhakoo, *ACS nano*, 2013, **7**, 6796-6805.
14. M. Chen and M. Yin, *Prog. Polym. Sci.*, 2014, **39**, 365-395.

15. X. Zhang, X. Zhang, S. Wang, M. Liu, L. Tao and Y. Wei, *Nanoscale*, 2013, **5**, 147-150.
16. X. Zhang, X. Zhang, B. Yang, J. Hui, M. Liu, Z. Chi, S. Liu, J. Xu and Y. Wei, *Polym. Chem*., 2014, **5**, 318-322.
17. T. Korten, W. Birnbaum, D. Kuckling and S. Diez, *Nano Lett.* 2012, **12**, 348-353.
18. M. Yin, J. Shen, G. O. Pflugfelder and K. Müllen, *J. Am. Chem. Soc.*, 2008, **130**, 7806-7807.
19. J. Li, K. Guo, J. Shen, W. Yang and M. Yin, *Small*, 2014, **10**, 1351-1360.
20. M. R. Kumar, R. A. Muzzarelli, C. Muzzarelli, H. Sashiwa and A. Domb, *Chem. Rev*., 2004, **104**, 6017-6084.
21. R. Jayakumar, M. Prabaharan, S. Nair, S. Tokura, H. Tamura and N. Selvamurugan, *Prog. Mater Sci.*, 2010, **55**, 675-709.
22. C. Sanjai, S. Kothan, P. Gonil, S. Saesoo and W. Sajomsang, *Carbohydr. Polym.*, 2014, **104**, 231-237.
23. V. Zamora-Mora, M. Fernández-Gutiérrez, J. S. Román, G. Goya, R. Hernández and C. Mijangos, *Carbohydr. Polym.*, 2014, **102**, 691-698.
24. J. Li, C. Ji, W. Yang and M. Yin, *Analyst*, 2013, **138**, 7289-7293.
25. Y. Sun, X. Ding, Z. Zheng, X. Cheng, X. Hu and Y. Peng, *Eur. Polym. J.*, 2007, **43**, 762-772.
26. E. Yemm, E. Cocking and R. Ricketts, *Analyst*, 1955, **80**, 209-214.
27. L. Ma, M. Liu, J. Chen, H. Liu, D. Cui and C. Gao, *Adv. Eng. Mater.*, 2009, **11**, B267-B274.
28. Z. Shi, K. Neoh, E. Kang, B. Shuter, S.-C. Wang, C. Poh and W. Wang, *ACS Appl. Mater. Interfaces*, 2008, **1**, 328-335.
29. L. Lou, K. Yu, Z. Zhang, B. Li, J. Zhu, Y. Wang, R. Huang and Z. Zhu, *Nanoscale*, 2011, **3**, 2315-2323.
30. L. P. Fernando, P. K. Kandel, J. Yu, J. McNeill, P. C. Ackroyd and K. A. Christensen, *Biomacromolecules*, 2010, **11**, 2675-2682.

